Acta Biochim Biophys Sin, 2016, 48(4), 395–398
doi: 10.1093/abbs/gmw006
Advance Access Publication Date: 27 February 2016
Lab Note

Lab Note

miRNAs associated with the malignant transformation of non-small cell lung cancer

Detao Wang[1], Qian Zhang[2], and Youxin Jin[1,3,*]

[1]School of Life Sciences, Shanghai University, Shanghai 200444, China, [2]Shenzhen Institutes of Advanced Technology, Chinese Academy of Sciences, Shenzhen 518055, China, and [3]State Key Laboratory of Molecular Biology, Institute of Biochemistry and Cell Biology, Institutes for Biological Sciences, Chinese Academy of Sciences, Shanghai 200031, China

*Correspondence address. Tel/Fax: +86-21-66137016; E-mail: yxjin@sibs.ac.cn

Lung cancer is the leading cause of cancer-related death, both in China and worldwide, with non-small cell lung cancer (NSCLC) accounting for ~80% of all lung cancers. Despite of improvements in clinical strategies, the 5-year survival rate after curative treatment is still very poor [1,2]. KRAS mutations were found to be significantly more frequent in adenocarcinoma patients [3]. The p53 transcription factor is a critical tumor suppressor, as evidenced by the observations that it is mutated in over half of all human cancers and that p53 null mice develop cancer with 100% penetrance [4]. Furthermore, the presence of KRAS mutations with p53/LKB1 loss confers worse outcomes in preclinical murine models and is predictive for resistance to selumetinib and docetaxel [5]. Therefore, to treat human NSCLC, identification of better targets based on background genotype has become an immediate goal of the utmost importance, and crucial for the development of new and more effective strategies.

MicroRNAs (miRNAs) are small noncoding RNA molecules that inhibit gene expression at the posttranscriptional level by binding to the 3′-untranslated region of target mRNAs [6]. In order to decipher the molecular mechanisms associated with the progression and development of NSCLC, identifying the targets of associated miRNAs is critical and the first step toward discovering new ways to treat lung cancer. Recent findings have highlighted a relevant role for miRNAs in the regulation of tumorigenesis events. Based on these premises, we sought to investigate the regulation network of miRNAs in NSCLC.

C57BL/6 mice, $KRAS^{+/+}$, $KRAS^{+/+}p53^{-/-}$, and $KRAS^{+/+}LKB1^{-/-}$ NSCLC mouse models were precious gifts from Dr Hongbin Ji (Shanghai Institutes for Biological Science, Shanghai, China). All the mice were maintained under specific-pathogen-free conditions, and animal experimentation was conducted in accordance with institutional guidelines [7]. miRNA solexa sequencing was performed by Beijing Genomic Institute Company (Beijing, China).

Human lung cancer cells (A549, Beas-2b, SPCA-1, and 95-D) were obtained from the Cell Bank, China Academy of Sciences (Shanghai, China). H1299 were purchased from the American Type Culture Collection (Manassas, USA). Beas-2b cells isolated from normal human bronchial epithelium was cultured in LHC-9 medium. A549 cells were cultured in F12K medium (Gibco, Gaithersburg, USA), and all the other lung cancer cells were cultured in RPMI-1640 medium (Gibco), supplemented with 10% fetal bovine serum (Hyclone, Logan, USA), 100 U/ml penicillin and 100 μg/ml streptomycin. All cells were cultured in a 5% CO_2 humidified incubator at 37°C.

Total RNA was extracted using Trizol regent (Invitrogen, Carlsbad, USA) following the manufacturer's instructions. The level of miRNA was quantified by quantitative reverse transcriptase-polymerase chain reaction (qRT-PCR) using SYBR green PCR master mixture (TaKaRa, Dalian, China). U6 snRNA was used as an endogenous reference for miRNAs. Results were calculated using relative quantification ($2^{-\Delta\Delta C_t}$) method. Primer sequences were as follows—U6 sense: 5′-CTCGCTTCGGCAGCACA-3′, antisense: 5′-AACGC TTCACGAATTTGCGT-3′; miR-96 sense: TTTGGCACTAGCAC ATTTTTGCT; miR-34a sense: TGGCAGTGTCTTAGCTGGTTGT; miR-199a-3p sense: ACAGTAGTCTGCACATTGGTTA. The antisense primer for miRNA was the universal primer, which was supplied by the TaKaRa.

Molecular targets for each miRNA were predicted by TargetScan Online tools. Gene ontology analysis of miRNA targets was performed using DAVID (http://david.abcc.ncifcrf.gov/home.jsp). KEGG pathway enrichment analysis was performed for target genes of the miRNAs. The R language clusterProfiler package was used for enrichment analysis, setting the threshold for the false discover rate as (p.adjust) <0.05.

The STRING 9.0 tool was used to analyze protein–protein interaction (PPI). The occurrence of PPI was recognized when the PPI required confidence score was >0.9. Cytoscape software was then used to build a PPI network map.

To identify miRNAs that were associated with the malignant NSCLC, a total of 710 miRNAs was analyzed using a NSCLC mouse model. Sample information is shown in **Supplementary Table S1**. Wild-type C57BL/6 lung tissue was used as a control. Only mouse lung cancer tissues activated with $KRAS^{+/+}$ were identified as carcinoid, and the mouse lung cancer model that was $KRAS^{+/+}$ activated with p53/LKB1

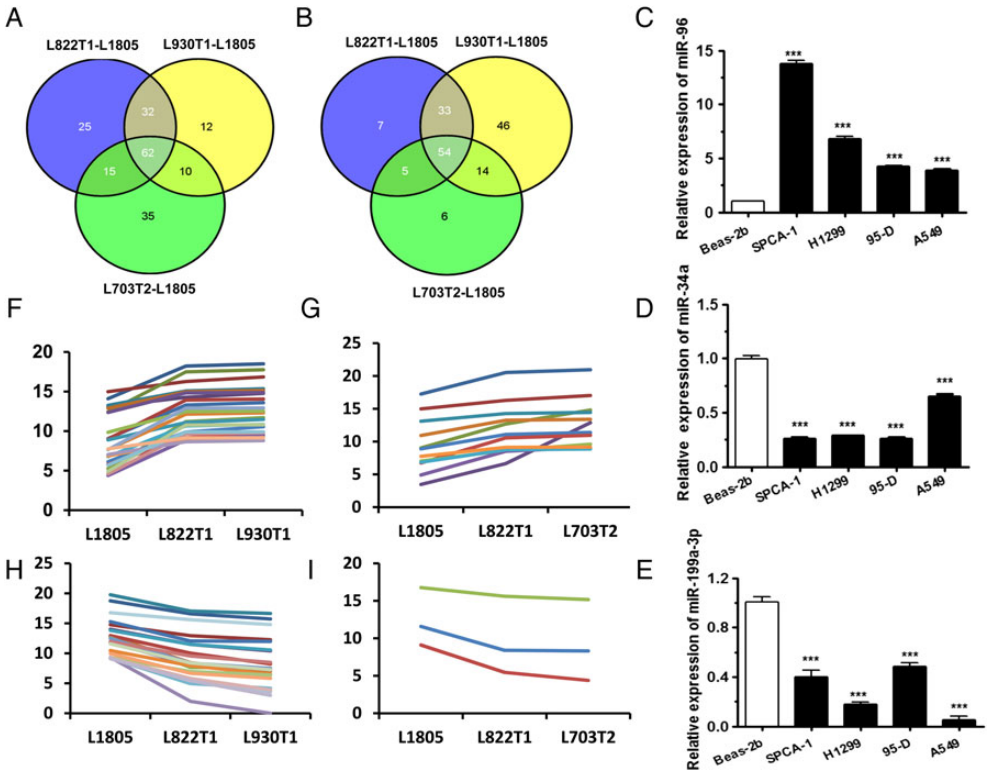

Figure 1. Differentially expressed miRNAs were analyzed in deep-sequence data of the NSCLC mouse model and identified in NSCLC cell line (A and B) Venn diagram of differentially expressed miRNA. (A) Upregulated miRNAs in the NSCLC mouse model. (B) Downregulated miRNAs in the NSCLC mouse model. (C–E) qPCR was performed to identify the upregulated and downregulated miRNAs in human NSCLC cell lines. All experiments were repeated in triplicate with similar results. U6 was used as an internal control. ***$P < 0.001$. (F–I) Cluster analyses of differentially expressed miRNAs. The horizontal axis represents the sample name, and ordinates represent the expression values (log 2). (F and G) The expression of miRNAs was continuously upregulated in carcinoid and malignant samples. (H and I) The expression of miRNAs was continuously downregulated in carcinoid and malignant samples.

loss was identified as a malignant tumor. According to the sample groups, we calculated the differential expression of miRNAs, using a threshold defined as $|\log FC| > 1$ and $P < 0.01$ (**Supplementary Table S2**). The number of differentially expressed miRNAs is shown in **Fig. 1**. There were 62 kinds of differentially expressed miRNAs, which were upregulated when compared with normal mouse lung tissues. Additionally, we found 54 kinds of differentially expressed miRNAs, which were downregulated. These results indicated that the miRNA expression profile is changed significantly along with the process of NSCLC aggravation.

Then we sought to further study the function of miRNAs in the progression of lung cancer. After filtering out those with read numbers <500 in the four samples, a total of 30 consistently upregulated or 24 consistently downregulated miRNAs in both the carcinoid and malignant groups were selected (**Fig. 1**).

To identify the differentially expressed miRNAs in human NSCLC cell line,qRT-PCR was performed to identify the upregulated miRNA (miR-96 as an example) and downregulated miRNA (miR-34a and miR-199a-3p as examples) in NSCLC cell lines. The expression of miR-96 in all NSCLC cell lines was found to be higher than that in the Beas-2b cells (**Fig. 1C**). Additionally, miR-34a and miR-199a-3p showed a lower expression in all NSCLC cell lines when compared with the Beas-2b cells (**Fig. 1D,E**). All these results were consisted of the deep-sequence data (data not shown).

To further expand our knowledge of the regulatory network associated with the aggressive malignant tissues, the online tool, TargetScan, was used to analyze the target genes of 30 upregulated miRNAs (**Fig. 1F,G**) and 23 downregulated miRNAs (**Fig. 1H,I**). Then, the R language package of cluster was used to perform KEGG pathway enrichment cluster analysis for the miRNAs with continuous upregulation and downregulation (**Fig. 2A,B**).

The top five upregulated miRNAs were mmu-miR-96 (25), mmu-miR-200b (19), mmu-miR-19b (19), mmu-miR-29a (12), and mmu-miR-29b (12). They showed the most enrichment for the corresponding KEGG pathway (note: numbers in parentheses represent the value enriched pathway term). Additionally, the results indicated that these five pathway terms are Axon guidance, the MAPK signaling pathway, the Wnt signaling pathway, chronic myeloid leukemia, and the ErbB signaling pathway (**Supplementary Table S3**).

The top five downregulated miRNAs were mmu-miR-195 (22), mmu-miR-497 (22), mmu-miR-199a-3p (9), mmu-miR-145 (8), and mmu-miR-503 (7). They showed the most enrichment for the corresponding KEGG pathway (note: numbers in parentheses represent the value enriched pathway term). Furthermore, the results obtained from the first five pathway terms were pathways in cancer, focal adhesion, regulation of the actin cytoskeleton, melanoma, and chronic myeloid leukemia (**Supplementary Table S4**).

PPI analysis was performed for the target genes of the five miRNAs with differential expression that were either continually upregulated or downregulated in NSCLC. The online tool, STRING, was used, setting combined score ≥0.9. The Cytoscape software was then used to generate a PPI network map by removing the subnetworks with less than five nodes (**Fig. 2C,D**).

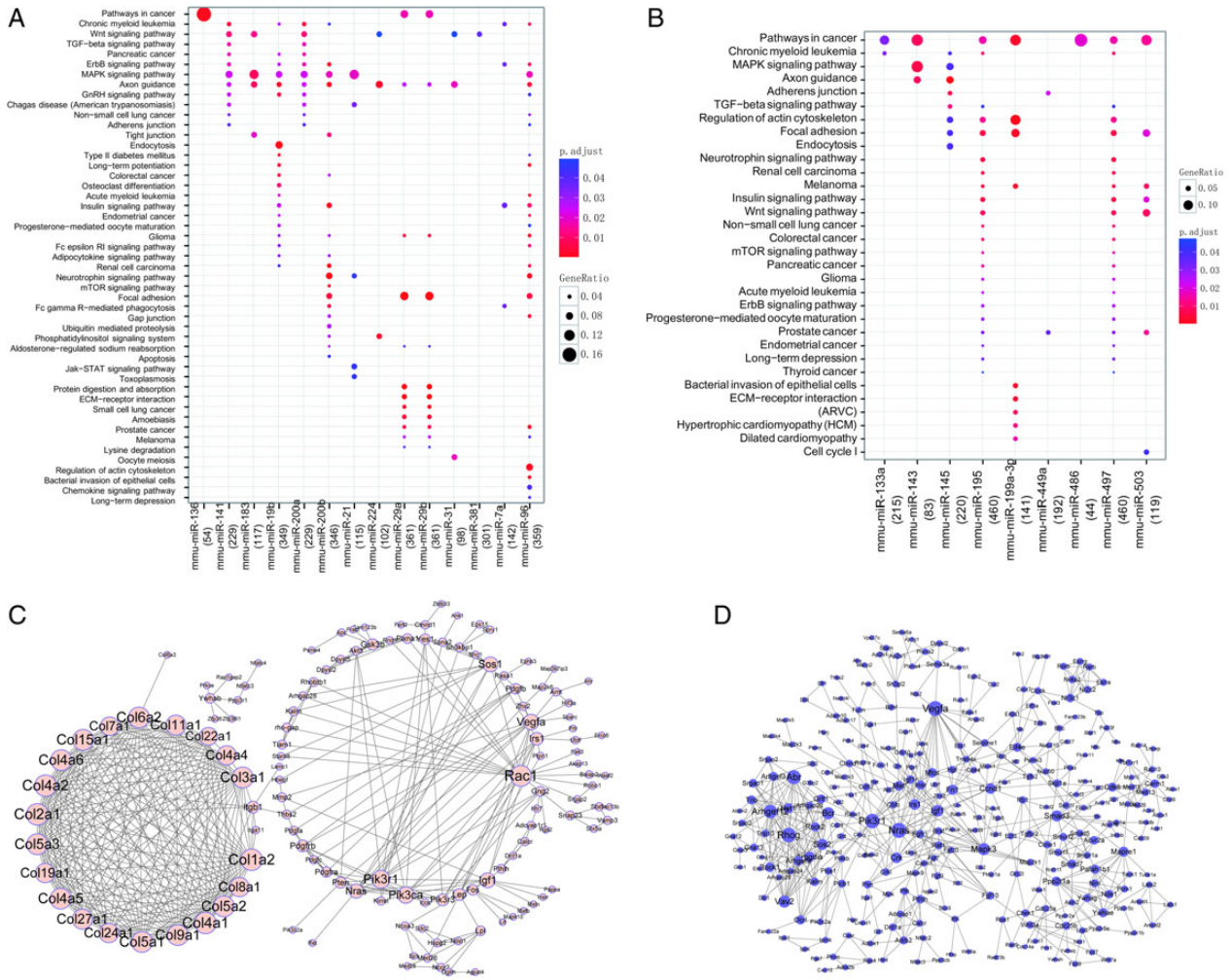

Figure 2. KEGG pathway enrichment analysis and PPI network for miRNAs with persistent differences (A) Upregulation. (B) Downregulation. The abscissa represents the different miRNAs; the brackets denote the number of target genes; the vertical coordinates represent the pathway term; p.adjust represents the enrichment *P*-value calculation of the correction value; gene ratio represents the enriched target gene proportion of the total target gene number. The PPI network of differentially upregulated (C) and downregulated (D) miRNA target genes. The join-point represents the protein, the horizontal line represents the interaction, and the size of the join-point represents the degree.

For the upregulated miRNA target genes, the data yielded 132 nodes (proteins) and 393 sides (**Fig. 2C**). The greatest connectivity of the top 20 proteins (**Supplementary Table S5**) had their function mainly enriched in two metabolic pathways: focal adhesion (Rac1, Col1a2, Col2a1, Col3a1, Col4a1, Col4a2, Col4a4, Col4a6, Col5a1, Col5a2, Col5a3, Col6a2, and Col11a1) and ECM-receptor interaction (Col1a2, Col2a1, Col3a1, Col4a1, Col4a2, Col4a4, Col4a6, Col5a1, Col5a2, Col5a3, Col6a2, and Col11a1). Of these top 20 proteins (**Supplementary Table S5**), only RAC1does not belong to the collagen family. Collagens are a super-family of extracellular matrix proteins that have a triple-helical domain as their common structural element and that play a role in maintaining the integrity of various tissues.

For the downregulated miRNA target genes, the data yielded 402 nodes (proteins) in total and 715 sides (**Fig. 2D**). The greatest connectivity of the top 20 proteins (**Supplementary Table S5**) had their function mainly enriched in pathways of cancer (Smad3, Bcr, Ccnd1, Fn1, Igf1, Mapk3, Pik3r1, Nras, Sos2, Crk, and Vegfa) and focal adhesion (Ccnd1, Fn1, Igf1, Mapk3, Pik3r1, Sos2, Crk, Vegfa, and Vav2).

Collectively, our results suggested that these upregulated and downregulated miRNAs constitute a complicated regulatory network involved in the process of lung cancer tumorigenesis. Further studies are needed to determine which of them can be used as biomarkers in the clinic.

Supplementary Data

Supplementary data is available at *ABBS* online.

Acknowledgement

We would like to thank Dr Yan Jin from Shenzhen Institutes of Advanced Technology, Chinese Academy of Sciences, for the assistance in the analysis of Solexa sequencing data.

Funding

This work was supported by the grants from the National Natural Science Foundation of China (No. 31170750), the National Basic Research Program of China (No. 2011CBA01105), the Shanghai Municipal Commission of Economy and Information (No.

11CH-08), and two foundations from the State Key Laboratory of Molecular Biology, the Institute of Biochemistry and Cell Biology, the Shanghai Institutes for Life Sciences, the Chinese Academy of Sciences.

References

1. Steuer CE, Behera M, Berry L, Kim S, Rossi M, Sica G, Owonikoko TK, *et al*. Role of race in oncogenic driver prevalence and outcomes in lung adenocarcinoma: results from the lung cancer Mutation Consortium. *Cancer* 2015. doi: 10.1002/cncr.29812.
2. Daniele S, Sandro B, Salvatore I, Alfredo F, Francesco F, Domenico G, Luca M, *et al*. Natural history of non-small-cell lung cancer with bone metastases. *Sci Rep* 2015, 5: 18670.
3. Sutherland KD, Song JY, Kwon MC, Proost N, Zevenhoven J, Berns A. Multiple cells-of-origin of mutant K-Ras-induced mouse lung adenocarcinoma. *Proc Natl Aca Sci USA* 2014, 111: 4952–4957.
4. Tseng SJ, Liao ZX, Kao SH, Zeng YF, Huang KY, Li HJ, Yang CL, *et al*. Highly specific *in vivo* gene delivery for p53-mediated apoptosis and genetic photodynamic therapies of tumour. *Nat Commun* 2015, 6: 6456.
5. Ou W, Ye S, Yang W, Wang Y, Ma Q, Yu C, Shi H, *et al*. Enhanced antitumor effect of cisplatin in human NSCLC cells by tumor suppressor LKB1. *Cancer Gene Ther* 2012, 19: 489–498.
6. Xu C, Zheng Y, Lian D, Ye S, Yang J, Zeng Z. Analysis of microRNA expression profile identifies novel biomarkers for non-small cell lung cancer. *Tumori* 2015, 101: 104–110.
7. Ji H, Ramsey MR, Hayes DN, Fan C, McNamara K, Kozlowski P, Torrice C, *et al*. LKB1 modulates lung cancer differentiation and metastasis. *Nature* 2007, 448: 807–810.